Use of the industrial X-ray computed microtomography to address scientific questions in developmental biology

Markéta Tesařová[1], Tomáš Zikmund[1], Markéta Kaucká[2,3], Igor Adameyko[2,3], Jozef Kaiser[1]

[1] Central European Institute of Technology, Brno University of Technology, CEITEC BUT, Purkyňova 123, 612 00 Brno, Czech Republic, e-mail: Marketa.Tesarova@ceitec.vutbr.cz, Tomas.Zikmund@ceitec.vutbr.cz, Jozef.Kaiser@ceitec.vutbr.cz

[2] Department of Physiology and Pharmacology, Karolinska Institutet, Nanna Svartz väg 2, Stockholm 17177, Sweden

[3] Department of Molecular Neurosciences, Center for Brain Research, Medical University of Vienna, Spitalgasse 4, Vienna, Austria 1090, Marketa.Kaucka@ki.se, Igor.Adameyko@ki.se

Abstract

X-ray computed microtomography (microCT) that allows to extract quantitative 3D information about various objects is already a well-established and widely used industrial technique for non-destructive testing, materials characterization and dimensional metrology. On the other hand, modern developmental biology requires both qualitative and quantitative three-dimensional information about the studied objects, which is not provided by conventional 2D imaging methods. In addition, the complexity of biological structures often requires a more comprehensive methodology to compare shapes and sizes. Our approach is to connect these two worlds, i.e. to apply procedures and analysis routinely used or developed for industrial computed tomography to address scientific questions in developmental biology. This approach, which is based on the long-term experience of the CEITEC BUT Brno micro/nanoCT research team on both, industrial and scientific application of X-ray microCT, brings new possibilities in imaging, data processing and evaluation of 3D biological models. Here we present 3D structures that were analysed by different approaches on the selected examples from developmental biology. In addition, quantitative analysis usually used in industry were applied to segmented 3D models e.g. wall thickness analysis of facial cartilage, shape comparisons of nasal capsules, automatic quantification of the cells in the salamander limb etc. A complete procedure consisting of staining, microCT measurement and subsequent data processing is discussed.

Keywords: microCT, 3D imaging, developmental biology, embryo

1 Introduction

One of the greatest enigmas of modern biology is how the shape diversity observed among living organisms is defined and controlled during its development and growth. For example, the embryo patterning is a highly dynamic process implicating multiple molecular mechanisms and cell interactions at the basis of organ formation. Defects in such cellular processes can affect the developmental programme and lead to congenital disorders [1-3]. To describe these processes in detail, the use of advanced imaging techniques is required. Today, due to the possibility of a fast measurement (in the order of minutes to hours) and simple sample preparation, this method finds its application both in the industry and various scientific fields including biology. Modern developmental biology requires both qualitative and quantitative 3D information about the studied objects, which is not provided by conventional 2D imaging methods. In addition, the complexity of biological structures often requires a comprehensive approach to compare shapes, sizes and volumes. To address this topic, numerous algorithms have been developed to study image segmentation and the evaluation of 3D volumes [4]. On the other hand, every topic requires its own approach and different parameters, which is hard to generalise for all 3D datasets. The goal of this work is to provide a connection between the industrial and biological approach.

2 Challenges of biological samples with CT

There are two basic approaches for imaging the soft tissues of biological samples. Because of a very similar attenuation coefficient of soft tissues (hydrogen, oxygen and carbon), staining chemical substances are used. In some cases, phase-contrast imaging is more convenient. However, the intensity projection image, acquired with a certain propagation distance between the sample and the detector, will always contain a mixture of contributions from both the absorption and the phase shifts in the sample. Thus, the combination of both methods is also used and it gives a good differential contrast and a higher resolution.

2.1 Staining

In the case of industrial CT systems, it is usually necessary to use contrasting agents (i.e. stains) to increase the X-ray absorption of soft tissues. There are various methods for staining biological samples. Staining methods that enable a high-contrast imaging of embryonic tissues at histological resolutions using a commercial CT system are demonstrated e.g. in [4-7]. The stains can usually be used after any common fixation and after storage in aqueous or alcoholic media, and on a wide variety of species. These methods establish the microCT imaging as a powerful tool for comparative developmental studies, embryo phenotyping, and quantitative modelling of development. On the other hand, the staining has some limitations: generally, it is usually applied only on *ex-vivo* samples; shrinking of tissue can appear with longer staining time; penetration of stains is limited etc.

Historically, the most successful contrast stain used for the CT imaging of soft tissues was osmium tetroxide. Its well-known tissue binding properties [8] make osmium tetra oxide a natural candidate for an X-ray contrast stain. On the other hand, the tissue penetration is limited, as it does not work well on the tissues that have been preserved in alcohol. Moreover osmium is volatile, toxic, and expensive to purchase and to dispose of [5].

The stains, based on phosphotungstic acid (PTA) and inorganic iodine, are easier to handle and much less toxic than osmium and produce high-contrast X-ray images for a wide variety of soft tissues [6]. PTA was utilised as a standard histological technique for light and electron microscopy thanks to its capability to increase the contrast of soft versus mineralised tissues or different types of soft tissues. PTA also confers a strong X-ray contrast when attached to the collagens, fibrils [9, 10] and to various other proteins. It is considered to be suitable for the visualising of soft connective tissue in general.

The various inorganic iodine stains usually produce similar results and are extremely simple to prepare and use. A big advantage of iodine staining is the rapid penetration of the sample in comparison with PTA. Also, its imparted contrast with various tissues is excellent. An example of brain imaging by iodine staining can be found in Figure 1 [7]. E.g., applying 1% iodine in 90% methanol for 24 hours (Figure 1H) enabled to clearly recognize some structures such as corpus callosum, anterior commissure, cerebral peduncle etc. using an industrial CT device (GE v|tome|x L 240). All the mentioned structures demonstrated well-defined edges in the μCT data. Moreover, the preparation time of the staining protocol was only one day in comparison with PTA staining that requires a much longer staining time (10 days).

To minimize the shrinking of the samples, it is needed to follow and optimise pre-stating steps for different types of the sample. The concentration and overall fixation and staining time depends on a dimension of a sample and on the type of tissue. Generally, the steps consist of tissue fixation, stabilization of the volume of a sample and finally dehydration. In particular, stabilization of sample's volume (e.g. use of acrylamide hydrogel solutions [11]) is an important step integrated into preparation of a sample as a prevention of a shrinking during staining in alcohol based solutions. The topic of optimisation of staining procedures has been already pursued and can be found e.g. in [5, 6, 11-14].

To summarise, contrast-enhanced CT by staining agents can produce quantitative, high-resolution, high-contrast volume images of soft tissues. Such images are expected to be useful in comparative, developmental, functional and quantitative studies of morphology [1, 2, 15].

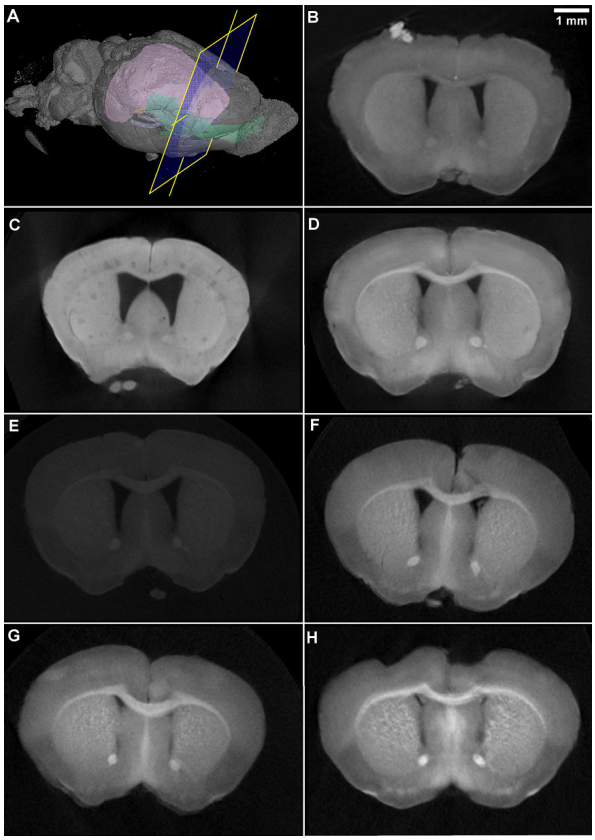

Figure 1: Comparison of the coronal sections of a brain following different staining protocols. A – Position of a coronal section on a 3D model, B – 1% PTA in 90% MeOH for 14 days, C – 1% PTA in 100% MeOH for 16 days, D – 1% PTA for 10 days + 1% iodine in 90% MeOH for additional 24h, E – 1% iodine in 100% EtOH for 24h, F – 1% iodine in 100% EtOH for 48h, G – 1% iodine in 100% EtOH for 7 days, H – 1% iodine in 90% MeOH for 24h. According to [7].

2.2 Phase contrast

The second approach is based on observing the phase change of X-rays after the interaction with the sample. By using the phase-sensitive techniques it is also possible to generate contrast in relation to the phase shifts imparted by the sample. These techniques also enable to extend the capabilities of X-ray imaging to the details that don't possess enough absorption contrast to be visualised only by measuring the decrease in X-ray intensity [16]. It is not possible to directly measure the phase of electromagnetic waves at optical frequencies. Phase-contrast imaging techniques use the phase perturbations introduced by the sample to modulate the intensity recorded at the image receptor, in such a way that these effects can be detected and interpreted. To observe phase change, the X-ray beam needs to have a high spatial coherence and parallel geometry [17]. These are typical characteristics of a synchrotron beam. However, under certain conditions, the industrial CT machines are capable of the phase-contrast imaging as well.

X-ray phase-contrast imaging techniques are evolving fast, and a large variety and different approaches exist (interferometry, grating based or analyser based methods etc.) Free-space propagation techniques are the ones requiring the simplest set-up and thus it is a method that can be used in industrial systems. The introduction of an appropriate propagation distance between the sample and the image detector can be sufficient to make the phase effects detectable.

3 Data analysis

With sufficient contrast imparted to soft tissues (Figure 2), linear and volumetric size changes in development can be readily measured, and comparisons of those measurements can be made between species or between control and genetically or experimentally manipulated specimens [1]. Because of the complex structures of biological samples, it is hard to find an appropriate general algorithm for evaluation of the data. Here, we take an advantage of analysis usually used in industry to answer biological questions. In this chapter, various samples from developmental biology are taken as an example for possible evaluation approaches to various types of tissue. To demonstrate the complexity of comparison of the samples, the following examples were selected: Wall thickness analysis of facial cartilage, shape comparison of mouse embryos' head, polarization of cells in developing limbs, volume determination of ossification centres and finally, 3D printing of various biological structures.

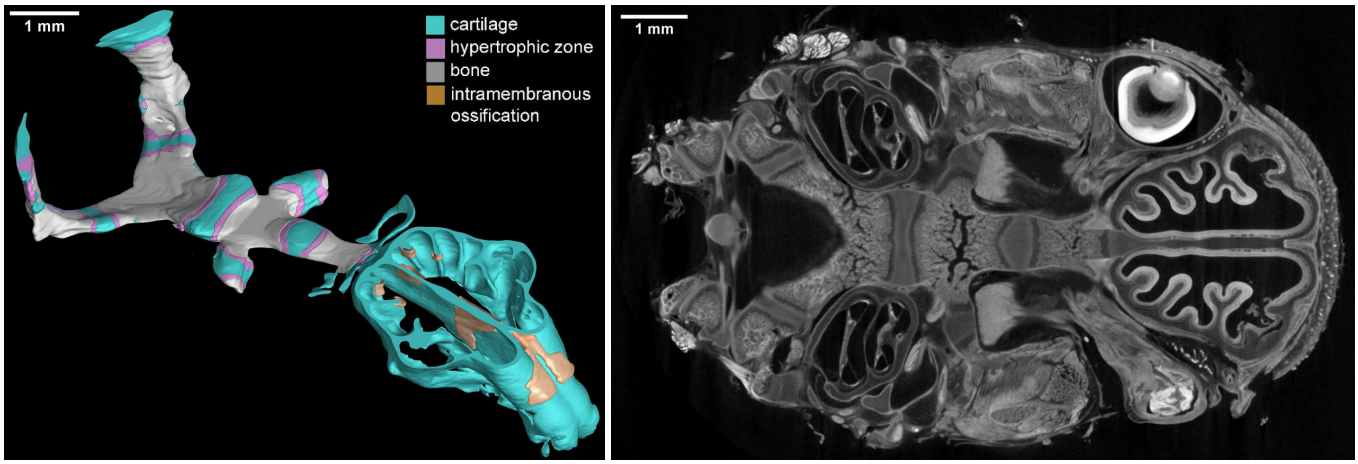

Figure 2: 3D visualization of ossifications and cartilage in the chondrocranium on a postnatal mouse 1 day after birth (in left). Original tomographic slice is in right [(Kaucka, et al., 2017)].

3.1 Wall thickness analysis

One of the sample properties that can help to precisely define the object is the thickness of its wall. Basically, two principles exist for the computing the thickness of the wall. The "ray method" which is ideal for typical near-parallel surfaces, and the "sphere method" which is suitable for measuring the thickness of curving and branching topologies. The basic principle of these two methods is illustrated in Figure 3. Then, this type of analysis processes a voxel data set for areas within a defined wall thickness interval. As a result of such an analysis, a detailed report of the detected wall thicknesses and a colour-coded data set can be computed.

Both of the mentioned methods are available in Volume Graphics software [18] and both methods have been tested in biology, specifically for measurement of the thickness of the cartilage of mouse embryos'chondrocranium. The main aim of this analysis was to answer the question whether the thickness of the chondrocranium changes across developmental stages of mouse embryos [1]. This structure consists of a near-parallel surfaces (nasal capsule, basisphenoid etc.) and also the round topologies (e.g. Meckel cartilage). Thus, it was not clear which method is more suitable and both methods have been tested.

The comparison of these two methods can be found in Figure 4. The wall thickness is the same for the near-parallel surfaces for both, ray and sphere method; however, some errors can be observed in the ray method round topologies. In this case, we can say that applying the sphere method is more suitable, because it is able to calculate the wall thickness for every part of the sample including flat, curving and branching topologies.

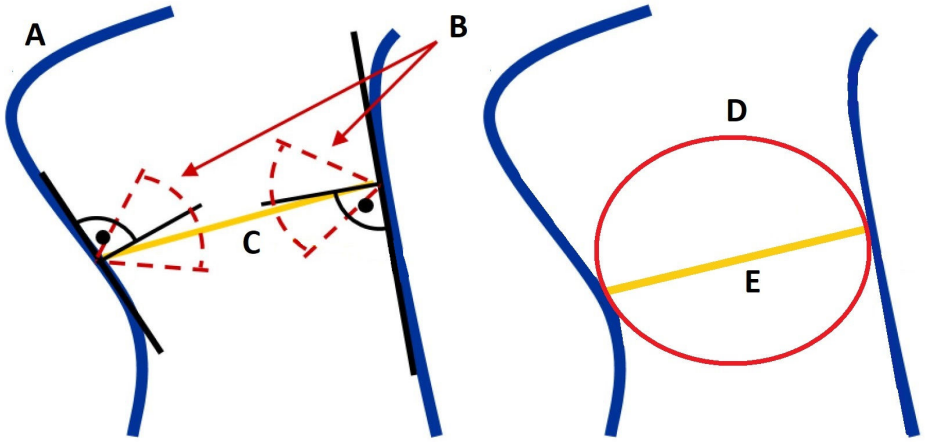

Figure 3: Basic principle of the ray (left) and sphere (right) method for wall thickness analysis in Volume Graphics software. A – surface of the object, B – search angle, C – measured distance for the ray method, D – fitted sphere, E – measured distance for the ray method [19].

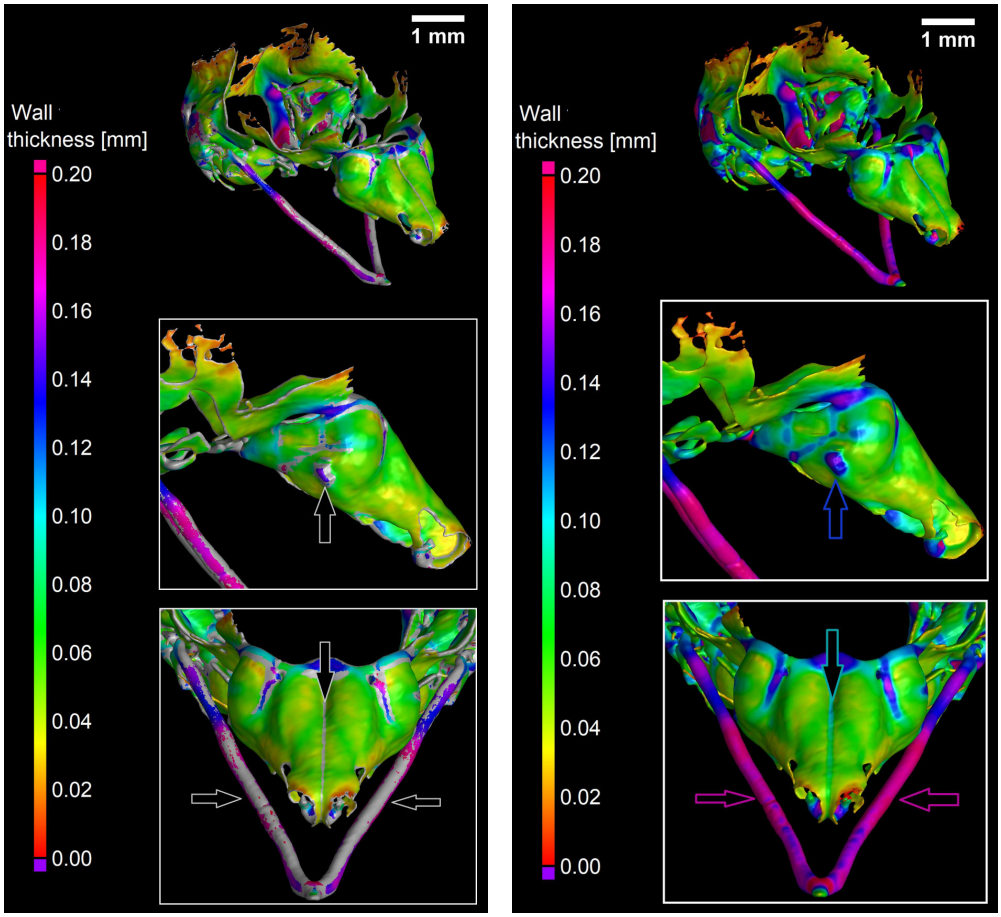

Figure 4: Comparison of ray (left) and sphere (right) method for wall thickness analysis in Volume Graphics software (VG 3.2) [18]. An example of cartilaginous chondrocranium of a mouse embryo at 15.5 days post fertilisation. The arrows on the 3D models show inaccuracy of the ray method for bended structures, e.g. for Meckel cartilage [19].

3.2 Shape comparison analysis

To perform a shape comparison analysis means to find appropriate morphometric methods. To conduct this type of analysis, many approaches can be taken. However, all of these approaches have their advantages and limitations. There is no single correct approach to morphometric that would be applicable to all problems. Approaches usually answer correctly the question being asked. However, they are correct or appropriate only in the context of that question. For this reason, it is critical to understand what different morphometric techniques do and to be aware of their respective limitations. Traditional morphometric relied on phenotypic measurements such as linear distances, angles, weights, and areas. However, most of the modern morphometric approaches are based on an analysis of landmarks. An assumption of landmark-based methods is that landmarks are homologous across individuals. A particular landmark should effectively correspond to the same point across the stages etc. Another approach is to transfer the model into triangular mesh and measure the distances between each triangle of the mesh.

We took an advantage of the long-term experience of our team on answering industrial questions, where shape comparison analysis needs to be utilized daily in a short-time. To compare tomographic data with e.g. a CAD is one of the typical task for industrial X-ray computed tomography.

The data of the heads was imported into one coordinate system and registered by the least squares method in VG Studio MAX 3.2 software. The result of the registration is shown in Figure 5. Then, all anatomical structures suitable for the position of the landmarks were overlapped (i.e. eyes, noses, dermal disparities etc.), thus the landmark-based methods are not very suitable. To compare the differences between the heads, the models were converted to the STL (stereolithography) model and then subjected to further analysis. The STL format is an example of the format mainly used for rapid prototyping, 3D printing and computer-aided manufacturing, and can also find its application in developmental biology. An STL file describes a raw, unstructured triangulated surface by the normal unit and vertices of the triangles using a 3D Cartesian coordinate system. The STL files were then imported to GOM Inspect software. This software is mainly used for the analysis of 3D measuring data for quality control, product development and production. The GOM software is used to evaluate 3D measuring data derived from GOM systems, 3D scanners, laser scanners, CTs and other sources [20]. By applying technical approaches, it was possible to calculate the distance between the triangles from mutant and control sample. Mutation of the embryo is described in [2]. The result of the analysis is shown in Figures 5 and 6.

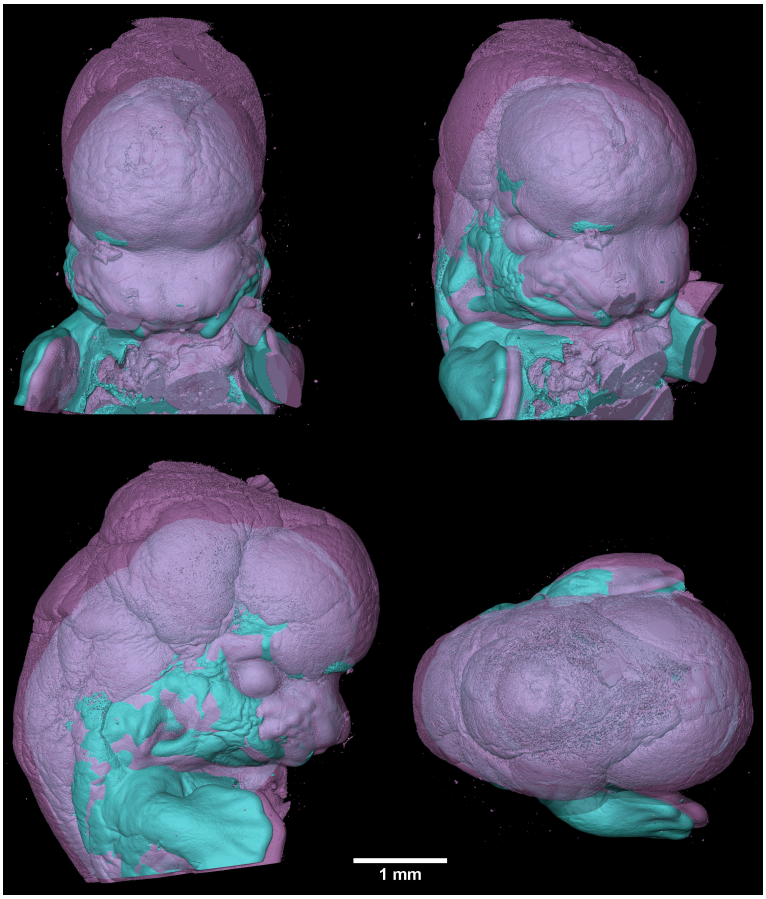

Figure 5: Location of the heads of the mouse embryo 12.5 days post fertilisation in the coordinate system used for further analysis. The blue colour represents the control embryo and pink colour represents the mutant.

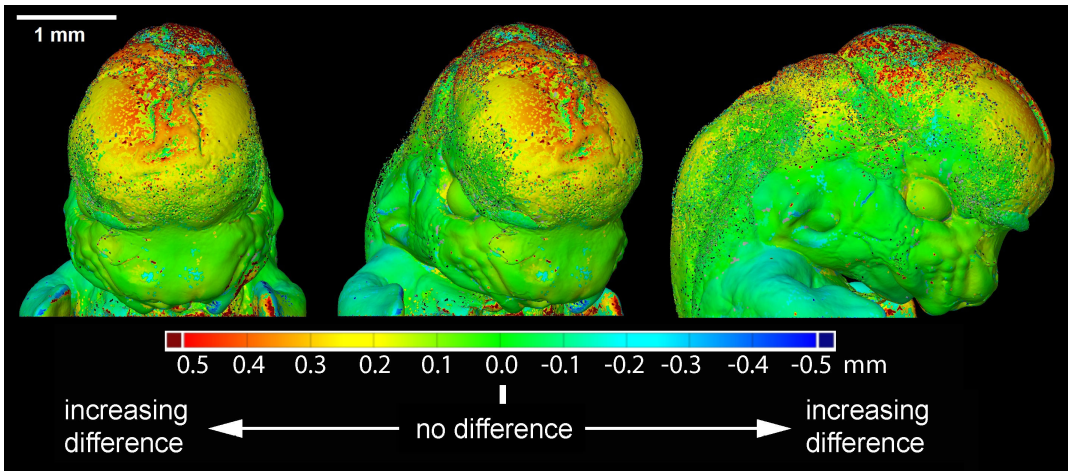

Figure 6: An example of quantification of 3D model by industrial approach. Comparison of the differences in the GOM inspect software. The green colour shows no deviation from the control embryo. According to [(Kaucka, et al., 2018)].

3.3 Volume determination – pore/inclusion analysis

The research focused on description of influence of Tmem107-/- protein null mutation on formation of primary cilia and development of craniofacial structures in mouse brings several requirements for 3D analysis [15]. The most important question was a need for comparison of ossification centres of a wild type, a heterozygote of mouse embryos 15.5 days post fertilization. These embryos were scanned without staining in order to detect ossification centres in the heads as these ossifications possess enough absorption contrast without need for further chemical preparation. Then, pore/inclusion analysis in VG Studio Max 3.1 was used to evaluate interconnection and volume of ossified tissue. Colour scale defines volume of each connected system of ossified tissue is demonstrated in Figure 7.

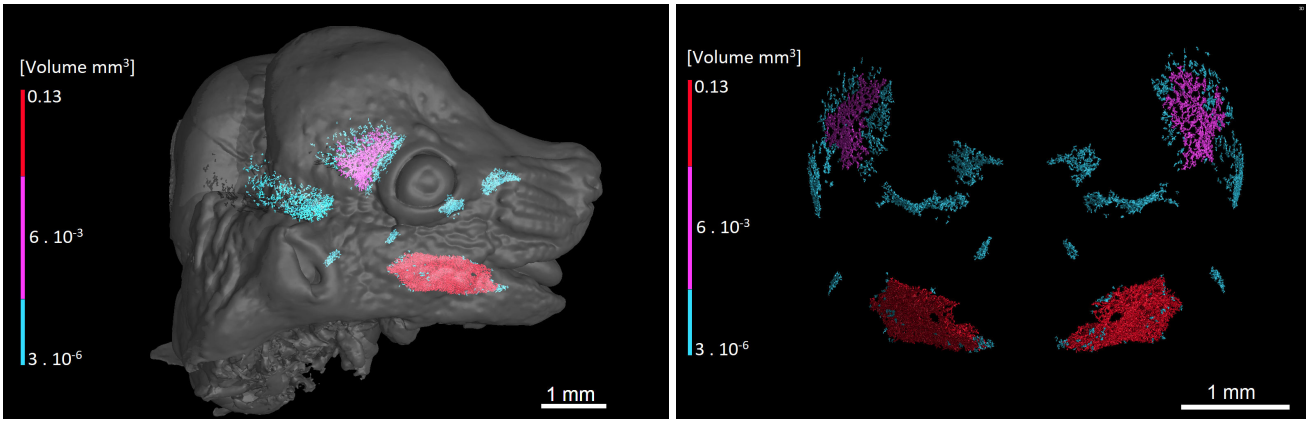

Figure 7: The inclusion analysis of ossification centres inside the head of mouse embryo 15.5 days post fertilisation. The semi-transparent 3D rendering of the whole head (left) and the detail of ossification centre (right). According to [15]

3.4 Fibre orientation – polarization of cells

It has been already demonstrated that it is possible to visualise cells by microCT method [21-25]. We have studied the regeneration and development of salamanders' limb because of their regeneration capabilities [21]. To describe the complex mechanism of regeneration, it is needed not only to visualise the cells, but also look to the data more quantitatively. Particularly, it was found out that by microCT imaging, the resolution and contrast enables to see the polarization of individual cells. To quantify what can be seen by human eyes, we utilized Fibre composite material analysis (FCMA) module which is implemented to VG Studio MAX software. The FCMA module has been designed to process voxel data sets to get information about fibre composite material, but we prove that it can be also used for biological objects as the chondrocytes in cartilage. The mapping of orientation of all chondrocytes within the cartilage provided important foundation for future inference of the oriented cell behaviour during cartilage shaping. This analysis demonstrated that the predominant orientation of chondrocytes in epiphyseal regions was different from rather central regions of the cartilage, where the cell density appeared low. Also, superficial chondrocytes were aligned with the developing surface of the cartilage (Figure 8) [21].

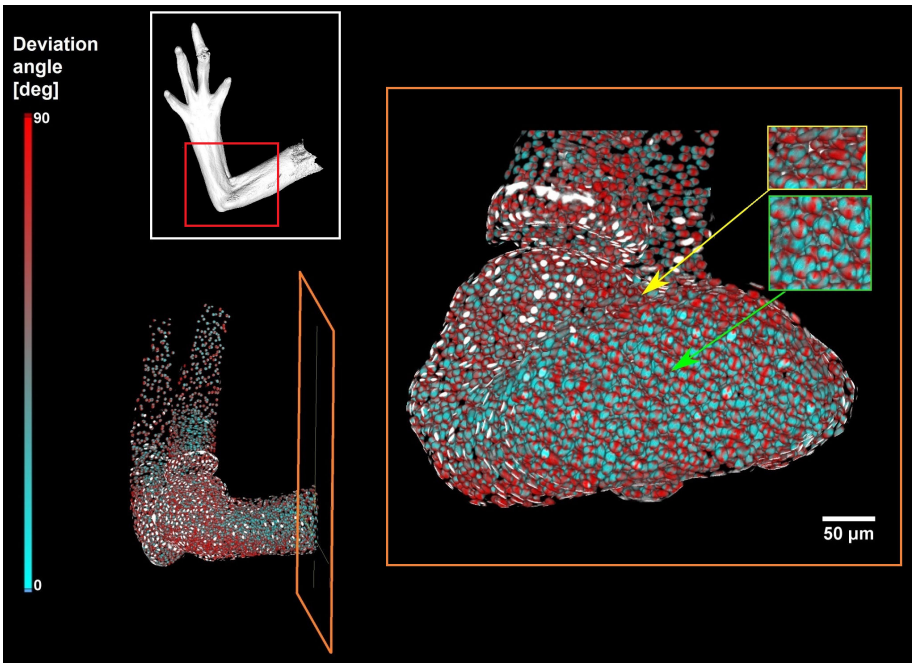

Figure 8: Polarization of the cells inside cartilage of embryonic salamander limb. Green and yellow window shows detail of orientation of the cells: Superficial chondrocytes near surface (yellow arrow) are aligned with the developing surface of the cartilage in the contrary of chondrocytes in the centre of the element (green arrow). According to [21].

3.5 3D printing

Despite there are many software-based ways for visualization of 3D data sets, having a real solid model of the studied object might give novel opportunities to fully understand not only technological and industrial methods but also biological processes. To create the scaled model of the observed sample is nowadays possible thanks to reverse-engineering methods. The straightforward combination of microCT with 3D printing is common in medical practice [26-28]. We have combined industrial microCT with 3D printing (printer ZPrinter 650) and we have demonstrated the full procedure of creating a real 3D object of the whole mouse embryo and different anatomical structures as spine or nasal capsule. The complete procedure consists of the staining, the microCT scanning combined by the advanced data processing and the 3D printing [4]. The examples of reverse-engineering by industrial microCT and 3D printing in biology can be seen in Figure 9. We were able not only to reverse-engineered cartilaginous spines of different mouse embryos, but we also combined these models with 3D rendering of the whole sample and by subtracting the segmented STL model from the 3D rendering of the whole body, we could see the shape and position of spine in the context of the whole sample.

Figure 9: 3D printing of the rendering of the whole body of mouse embryo with projected spine (left), developmental stage is E15.5. The individual spines with pelvis of mutant and control embryo (right).

4 Material and Methods

4.1 Preparation of the sample

After excision, the samples were fixed with 4% formaldehyde in phosphate buffer saline (PBS) for 24 hours at +4 ◦C. The samples were then washed with PBS and dehydrated by ethanol grade (30%, 50%, 70%), each concentration for 1 day. Experimentally, the best tissue contrast and penetration with PTA was found. Therefore, most of the samples were transferred from 70% ethanol to an ethanol-methanol-water mixture (4:4:3) and then into 80% and 90% methanol, each bath for 1 hour. After that, a 0.7% PTA-methanol solution was used to stain the sample for 6 days and exchanged each day with a fresh one. The staining was followed by rehydration of the sample in methanol grade series (90%, 80%, 70%, 50% and 30%) to end up in sterile distilled water. For the stability of microCT measurement, the sample was embedded in 1% agarose gel and placed in a plastic tube to avoid the motion artefacts during CT scanning.

4.2 Tomographic measurement

The plastic tube was fixed on a plastic rod with a silicone gun. The rod was mounted in the chuck which provides the position of the sample in the rotation axis. The microCT was performed at industrial CT machine GE v|tome|x L 240 in an air-conditioned cabinet (21 °C) at acceleration voltage from 60-80 kV and tube current 200-220 μA according to size of the sample. The data was acquired using a flat panel detector DXR250 with 2048 × 2048 pixels, 200 × 200 μm^2 pixel size. Exposure time was determined from 500 to 900 ms and 3 images were averaged for reducing the noise. 1800-2200 projections were taken over 360◦. The tomographic reconstruction was done using the software GE phoenix datos|x 2.0 (GE Sensing & Inspection Technologies GmbH, Germany) with an isotropic voxel size of 1-10 μm.

4.3 Data analysis

Reconstructed slices were further analysed using the different type of software: VG Studio Max 2.1 – 3.2, GOM Inspect and Avizo. More details can be found in [4, 19, 21].

Acknowledgements

This research was carried out under the project Czech Science Foundation GACR 17-14886S and CEITEC 2020 (LQ1601) with financial support from the Ministry of Education, Youth and Sports of the Czech Republic under the National Sustainability Programme II and CEITEC Nano Research Infrastructure (MEYS CR, 2016–2019).

References

[1] M. Kaucka et al., Oriented clonal cell dynamics enables accurate growth and shaping of vertebrate cartilage, eLife. 6 (2017) e25902.

[2] M. Kaucka et al., Signals from the brain and olfactory epithelium control shaping of the mammalian nasal capsule cartilage, eLife. 7, (2018) e34465.

[3] M. Kaucka et al., Analysis of neural crest–derived clones reveals novel aspects of facial development, Science Advances. 2 (2016) 1-16.

[4] M. Tesařová, T. Zikmund, M. Kaucká, I. Adameyko, J. Jaroš, D. Paloušek, D. Škaroupka, J. Kaiser, Use of micro computed-tomography and 3D printing for reverse engineering of mouse embryo nasal capsule, Journal of Instrumentation. 11 (2016) C03006-C03006.

[5] B. Metscher, MicroCT for comparative morphology: simple staining methods allow high-contrast 3D imaging of diverse non-mineralized animal tissues, BMC Physiology. 9 (2009) 1-14.

[6] B. Metscher, MicroCT for developmental biology: A versatile tool for high-contrast 3D imaging at histological resolutions, Developmental Dynamics. 238 (2009) 632-640.

[7] T. Zikmund, M. Novotná, M. Kavková, M. Tesařová, M. Kaucká, B. Szarowská, I. Adameyko, E. Hrubá, M. Buchtová, E. Dražanová, Z. Starčuk, J. Kaiser, High-contrast differentiation resolution 3D imaging of rodent brain by X-ray computed microtomography, Journal of Instrumentation. 13 (2018) C02039-C02039.

[8] J. Kiernan, Histological and Histochemical Methods: theory and practice. Pergamon Press, 1981.

[9] T. Nemetschek, H. Riedl, R. Jonak, Topochemistry of the Binding of Phosphotungstic Acid to Collagen, Journal of Molecular Biology, 133 (1979) 67-83.

[10] V. Constantine, R. Mowry, Selective Staining of Human Dermal Collagen, Journal of Investigative Dermatology. 50 (1968) 414-8.

[11] M. Wong, S. Spring, R. Henkelman, R. Morishita, Structural Stabilization of Tissue for Embryo Phenotyping Using Micro-CT with Iodine Staining, PLoS ONE. 8 (2013) e84321.

[12] X. Li, N. Anton, G. Zuber, T. Vandamme, Contrast agents for preclinical targeted X-ray imaging, Advanced Drug Delivery Reviews. 76 (2014) 116-133.

[13] E. Pauwels, D. Van Loo, P. Cornillie, L. Brabant, L. Van Hoorebeke, An exploratory study of contrast agents for soft tissue visualization by means of high resolution X-ray computed tomography imaging, Journal of Microscopy. 250 (2013) 21-31.

[14] P. Gignac et al., Diffusible iodine-based contrast-enhanced computed tomography (diceCT): an emerging tool for rapid, high-resolution, 3-D imaging of metazoan soft tissues, Journal of Anatomy.228 (2016) 889-909.

[15] P. Cela, M. Hampl, N. Shylo, K. Christopher, M. Kavkova, M. Landova, T. Zikmund, S. Weatherbee, J. Kaiser, M. Buchtova, M. Ciliopathy Protein Tmem107 Plays Multiple Roles in Craniofacial Development, Journal of Dental Research. 97 (2017) 108-117.

[16] M. Endrizzi, X-ray phase-contrast imaging, Nuclear Instruments and Methods in Physics Research Section A: Accelerators, Spectrometers, Detectors and Associated Equipment. 878 (2018) 88-98.

[17] Kalasová, D., Implementation of phase contrast in X-ray Computed Tomography. Master's thesis (2016).

[18] Volume Graphics. https://www.volumegraphics.com 2018 (accessed 25 November 2018).

[19] Tesařová, M. Implementation of industrial X–ray computed microtomography in developmental biology. Master's thesis (2018).

[20] GOM Inspect Software: Evaluation Software for 3D Measurement Data. https://www.gom.com/3d-software/gom-inspect.html 2018 (accessed 6 June 2018).

[21] M. Tesařová, L. Mancini, A. Simon, I. Adameyko, M. Kaucká, A. Elewa, G. Lanzafame, Y. Zhang, D. Kalasová, B. Szarowská, T. Zikmund, M. Novotná, J. Kaiser, A quantitative analysis of 3D-cell distribution in regenerating muscle-skeletal system with synchrotron X-ray computed microtomography, Scientific Reports. 8 (2018) 14145.

[22] L. Vojtová, T. Zikmund, V. Pavliňáková, J. Šalplachta, D. Kalasová, E. Prosecká, J. Brtníková, J. Žídek, D. Pavliňák, J. Kaiser, The 3D imaging of mesenchymal stem cells on porous scaffolds using high-contrasted x-ray computed nanotomography, Journal of Microscopy. (2018) *in print*.

[23] R. Zehbe, A. Haibel, C. Brochhausen, U. Gross, C. Kirkpatrick, H. Schubert, Characterization of oriented protein-ceramic and protein-polymer-composites for cartilage tissue engineering using synchrotron μ-CT, International Journal of Materials Research. 98 (2007) 562-568.

[24] R. Zehbe, A. Haibel, H. Riesemeier, U. Gross, C. Kirkpatrick, H. Schubert, C. Brochhausen, Going beyond histology. Synchrotron micro-computed tomography as a methodology for biological tissue characterization: from tissue morphology to individual cells, Journal of The Royal Society Interface. 7 (2009) 49-59.

[25] S. Hieber, C. Bikis, A. Khimchenko, G. Schweighauser, J. Hench, N. Chicherova, G. Schulz, B. Müller, Tomographic brain imaging with nucleolar detail and automatic cell counting, Scientific Reports. 6 (2016) 32156.

[26] F. Rengier, A. Mehndiratta, H. von Tengg-Kobligk, C. Zechmann, R. Unterhinninghofen, H. Kauczor, F. Giesel, 3D printing based on imaging data: review of medical applications, International Journal of Computer Assisted Radiology and Surgery. 5 (2010) 335-341.

[27] E. Huotilainen, M. Paloheimo, M. Salmi, K. Paloheimo, R. Björkstrand, J. Tuomi, A. Markkola, A. Mäkitie, Imaging requirements for medical applications of additive manufacturing, Acta Radiologica. 55 (2014) 78-85.

[28] A. Hespel, R. Wilhite, J. Hudson, Applications for 3D printers in veterinary medicine, Veterinary Radiology & Ultrasound. 55 (2014) 347-358.